2012 Intelligent Vehicles Symposium
Alcalá de Henares, Spain, June 3-7, 2012

Multipath Detection with 3D Digital Maps for Robust Multi-Constellation GNSS/INS Vehicle Localization in Urban Areas

Marcus Obst, Sven Bauer, Pierre Reisdorf and Gerd Wanielik

Abstract— **Reliable knowledge of the ego position for vehicles is a crucial requirement for many automotive applications. In order to solve this problem for satellite-based localization in dense urban areas, multipath situations need to be handled carefully. This paper proposes a lightweight multipath detection algorithm which is based on dynamically built 3D environmental maps. The algorithm is evaluated with simulated and real-world data. Furthermore, it is applied to a combined GPS and GLONASS system in combination with a loosely coupled integration of odometry measurements from the vehicle.**

I. Introduction

The reliable knowledge of the ego position of vehicles is an important requirement for many automotive applications. Only with exact positioning—both in terms of accuracy and integrity—Advanced Driver Assistance Systems (ADASs) like blind spot detectors or green driving assistants can be realized and successfully deployed. During the last years, satellite-based positioning sensors like the Global Positioning System (GPS) have emerged as standard solution for the localization task. Low-cost single frequency GPS receivers are nowadays integrated in almost any mid-range vehicle. While for most comfort applications (e.g. navigation systems) the typical performance of standalone Global Navigation Satellite System (GNSS) localization with app. 20 m is sufficient, good positioning quality cannot be assumed in general. For example, in dense urban areas where GPS signals may be blocked by buildings or vegetation, the localization accuracy may decrease dramatically.

Moreover, the so called multipath effect of GNSS signals has to be considered carefully. If a satellite signal is subject to multipath—which can be caused by reflections on buildings—an additional time delay is introduced. This unhandled delay noticeably degrades the positioning accuracy and thus typically violates the estimated confidence interval, which is especially important for safety applications.

In this paper, a lightweight and real-time capable multipath detection algorithm for GNSS signals which uses a dynamically created 3D environmental map is presented. Within the 3D map, a raytracing algorithm is used to detect and predict potentially multipath subjected observations. The proposed algorithm can be used as an add-on for classical positioning algorithms and is demonstrated in a multi-constellation GPS and GLONASS environment. The GNSS fixes are fused with the in-vehicle odometry measurements in a loosely coupled GNSS/INS manner.

All authors are with the Professorship of Communications Engineering, Chemnitz University of Technology, Chemnitz, Germany, e-mail: firstname.lastname@etit.tu-chemnitz.de

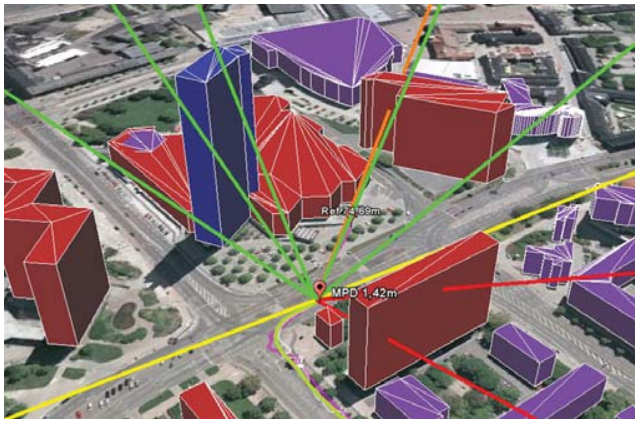

Fig. 1. Typical multipath situation in urban environment—here shown for inner city ring of Chemnitz, Germany. The direct line-of-sight of the vehicle GNSS receiver to some satellites is blocked by buidings (red). Pseudoranges which are directly observable are indicated by green lines.

Furthermore, the algorithm is designed to explicitly consider and handle uncertainties in the digital maps. The proposed algorithm is evaluated with simulated and real-world data from an urban test drive and compared to a highly accurate reference sensor system.

The paper is structured as follows: Section II gives a brief introduction of the state of the art and related work. In section III the fundamentals of GNSS positioning for single and multi-constellation systems are introduced. Furthermore, this section contains a brief overview about probabilistic filtering and vehicular motion models. In the subsequent section IV, the implementation of the 3D environmental model as well as the multipath detection algorithm is presented. The evaluation methodology which includes the experimental setup and simulation environment is described in section V.

Section VI contains detailed quantitative results of the multipath detection algorithm evaluation. The paper concludes with a discussion and an outlook for future work in section VII.

II. State of the Art & Related Work

Different approaches for dedicated detection of GNSS multipath situations can be found in literature. For example, high quality antennas, e.g. with choke ring design or the usage of antenna arrays can improve reception performance even under difficult conditions [1].

If multipath affected pseudoranges are considered as outliers, the detection can be done by the *Receiver Autonomous Integrity Monitoring* algorithm (RAIM) and its extensions

978-1-4673-2118-1/$31.00 ©2012 IEEE

[2]. However, classical RAIM is limited to assume and detect only one outlier within the pseudorange set. It is therefore not fully appropriate for urban multipath situations, where even more than one observation may be affected.

In [3], a multipath detection algorithm based on an additional infrared camera is introduced. There, the camera is mounted on the vehicle roof and observes the sky for buildings blocking the direct line-of-sight between the antenna and the GPS satellites.

Based on the publicly available elevation data of the *Shuttle Radar Topography Mission* (SRTM), in [4] a static digital elevation and azimuth map is proposed and used for a sophisticated modeling of GPS signals.

Another related work attempts to autonomously detect multipath signals in urban environments with an integrated Bayesian integrity monitoring algorithm and shows its feasibility through simulations [5].

While the previous references mainly investigated the multipath detection and mitigation, in [6] trials for GPS/GLONASS receivers are presented. However, even if the authors could show a benefit for the positioning performance in urban areas, they do not address multipath explicitly.

In contrast to the previously described methods, the scope of this paper is to introduce a GNSS multipath detection algorithm which is based on raytracing within a dynamically built 3D environment map. The proposed algorithm will be real-time capable and has low computational demands. Furthermore, no additional physical sensors are required. Finally, the algorithm is designed to be compatible with GPS and GLONASS and can be easily adapted to other available GNSSs. It can be used as an add-on for least-squares or Kalman filter based localization algorithms.

III. Fundamentals

A. GNSS Positioning and Multipath

Normally, the determination of a GNSS position is based on taking several raw GNSS measurements of one epoch and processing them through a least-squares estimator. The raw observations—often called pseudoranges—are time of flight measurements between the receiver antenna and the visible satellites. As the position on earth is fully described by a three dimensional coordinate, at least three pseudoranges are needed for the localization solution in theory. Due to the unsynchronized receiver clock, a time bias between the satellites and the user receiver has to be considered, too. Therefore, the unknown clock offset needs to be estimated through a fourth pseudorange observation.
According to [7] the pseudorange ρ can be modeled as:

$$\rho = r + c(dt - dT) + d_{\text{ion}} + d_{\text{trop}} + d_{\text{eph}}. \tag{1}$$

In the given equation, c is the speed of light and r represents the true geometric distance between the receiver and the satellite. The satellite clock offset dT can be taken from the broadcasted ephemeris and is therefore assumed to be known in advance for each satellite, while the receiver clock offset dt remains unknown. Furthermore, the pseudorange is subject to a propagation delay caused by the ionosphere d_{ion} and troposphere d_{trop}. Since the satellite position derived from the ephemeris may be inaccurate to a certain extent, the error term d_{eph} is introduced. Other errors like measurement noise of the receiver or local phenomena like multipath are not covered by this model.

If at least four pseudoranges are available the receiver state

$$x_{\text{receiver}} = \begin{pmatrix} x & y & z & dt \end{pmatrix}^{\text{T}} \tag{2}$$

can be solved through a least-squares algorithm or a Bayes filter implementation like the Kalman filter. Unaccounted errors within the pseudoranges will normally lead to a bias in the final absolute position estimate.

As indicated above, this pseudorange model does not consider local multipath effects. In urban areas, multipath typically can increase the pseudorange by up to 150 m and therefore significantly modify the positioning solution. An extension of (1) with an additive multipath term d_{mul} is given by:

$$\rho = r + c(dt - dT) + d_{\text{ion}} + d_{\text{trop}} + d_{\text{eph}} + d_{\text{mul}}. \tag{3}$$

Unfortunately, it is hard to exactly know or estimate d_{mul} in advance, as this term heavily depends on the local environment of the receiver antenna. In the paper at hand, the presence of the term d_{mul} will be detected by a 3D model in combination with raytracing.

B. Multi-Constellation GNSS Positioning

In this paper two different GNSSs, i.e. the American GPS and the Russian GLONASS system, are used simultaneously. If two or more GNSSs are used in parallel, this is typically referred as multi-constellation positioning. As indicated above in (2), in addition to the antenna position, a time offset between the receiver and the satellite system time needs to be estimated for each satellite system. Therefore, another time offset has to be calculated if GPS and GLONASS are used at the same time. The complete system state to estimate for a combined GPS/GLONASS algorithm is described by

$$x_{\text{receiver}} = \begin{pmatrix} x & y & z & dt_{\text{GPS}} & dt_{\text{GLONASS}} \end{pmatrix}^{\text{T}}, \tag{4}$$

where x, y and z denote the receiver position in Earth-Centered, Earth-Fixed (ECEF) coordinates. The time offset of the local receiver to the GPS system time is dt_{GPS}, and for GLONASS dt_{GLONASS}. It should be noted that for a combined positioning solution, the minimum number of pseudorange observations increases to five, e.g. four GPS pseudoranges are used to estimate the ECEF position and GPS time offset, and one GLONASS pseudorange is used for the determination of the GLONASS time offset [8].

C. Vehicular Motion Models

A motion model can be used to describe the physical constrains which apply to a moving vehicle. Thus, the simplest model assumes a linear or a uniformly accelerated motion. In literature, there exists a large number of different motion models, e.g. in [9] a systematical overview of the most common vehicular motion models is given. There, the models

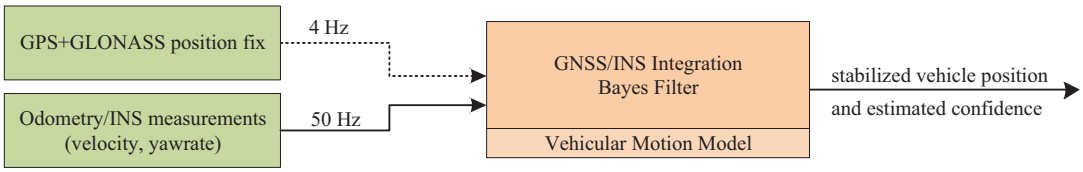

Fig. 2. Schematic description of a loosely coupled GNSS/INS integration method as used in the proposed system. The uncertain asynchronous sensor observations are fused by a Bayes filter implementation which utilized a vehicular motion model to account for physical constrains. Normally, the combined GPS & GLONASS position fix is generated with 4 Hz. If the multipath detection leaves less than four satellite measurements, no GNSS fix can be calculated. In this case, the filter update for the GNSS fix is skipped (indicated by the dotted line).

are empirically evaluated in terms of suitability for advanced driver assistance systems (ADASs).

Together with a Bayes filter, a motion model can be used as state space model to smooth and stabilize the positioning solution of a GNSS-based localization algorithm. It has to be highlighted that such a model is crucial to predict the vehicle pose in time. This is especially important when GNSS fixes are not available or of bad quality due to an urban canyon which blocks the reception of satellite signals.

In this work, the *Constant Turn Rate and Velocity* (CTRV) model from [9] is used. The state space ${}^{\text{CTRV}}\mathbf{x}$ to estimate is

$$ {}^{\text{CTRV}}\mathbf{x} = \begin{pmatrix} x & y & \vartheta & v & \omega \end{pmatrix}^{\text{T}}. \tag{5} $$

Here, x and y denote the Cartesian two dimensional position (e.g. in UTM coordinates), while ϑ is the heading. The dynamic parameters v and ω represent the velocity and the yaw rate.

In this paper, the Bayes filter was implemented via an *Unscented Kalman Filter* (UKF) [10] which allows non-linear state transition equations and measurement models. In contrast to the *Extended Kalman Filter* (EKF), the UKF does not require a Jacobian matrix which often allows easier implementation during prototyping. Fig. 2 shows a schematic description of the Bayes filter for loosely coupled GNSS/INS integration. For the sake of compactness, the details of the Bayes algorithm are not discussed further. In [11], a comprehensive discussion of this topic can be found.

D. Sensor Models

Similar to the motion models, there is also a variety of sensor models which describe the transformation from the system state space to the measurement space. In this paper, only sensors are used which directly observe elements of the state vector. That is, the INS/odometry sensor generates yaw rate and velocity measurements, while the GNSS algorithm emits a position fix.

IV. Implementation

A. 3D Environment Model

To detect and predict GNSS multipath situations in urban areas without any additional hardware sensors, a 3D representation of the surrounding of the receiver antenna is proposed. Afterwards, a raytracing algorithm is used to examine whether satellite signals are reflected or blocked. In the following section, the generation of the 3D environmental map is explained in detail.

1) Digital Road Map: For the sake of simplicity, the building layouts are taken from 2D road maps. Even if there are many internet map providers like *Google Maps* or *Bing*, an easy to access interface is often missing. Therefore, it was decided to use the publicly available *OpenStreetMap* (OSM) service. Within the OSM database, building layouts are contained as separate polygons. They can be easily accessed by a well-documented online API which allows an efficient geo-referenced query style. Furthermore, the OSM data can be downloaded in the *Shapefile* format for offline use. For this work, the area of the test drive (Saxony, Germany) was downloaded from [12] and imported to a local *Structured Query Language* (SQL) database with a spatial extension.

2) 3D Building Models: To extrude the 3D building models from the previously described building layouts, the exact height in relation to the road surface is necessary. Unfortunately, the OSM database does not entirely contain this information. Hence, the building height needs to be extracted from another source. In [4], the publicly available elevation data from the *STS-99 Shuttle Radar Topography Mission* was used. Even if this database is a comprehensive representation of the whole world, it does not include the height information with an appropriate resolution for this work. Therefore, geo information, i.e. digital terrain and elevation model, from the land surveying office of Saxony (GeoSN) with a horizontal resolution of 2 m and an accuracy of 0.2 m are used instead. Similar to the processing of the OSM data, the elevation information is converted to a common coordinate system and imported in the geo-referenced database.

The actual generation of the 3D environment around the receiver antenna is done dynamically during the positioning step. By that approach, only the required building models need to be created which efficiently lowers the computational load. For this purpose, the following steps are performed:

1) Query all building layouts within an area of 500 m around the current antenna position from the database.
2) For each building layout, generate a number of mesh points.
3) For each mesh point, lookup the height from the digital terrain model. The smallest value represents the base of the building.
4) For the same mesh points, lookup the height from the digital elevation model. The larges value indicates the top of the building.
5) Calculate absolute building height from the two previously estimated mesh points.

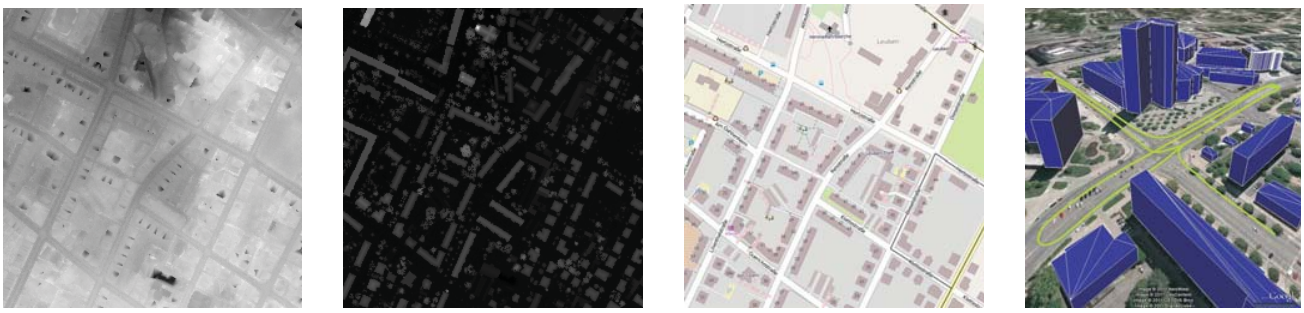

(a) Digital Terrain Model (b) Digital Elevation Model (c) OpenStreetMap (d) Final 3D Model

Fig. 3. Generation of 3D model from different digital map sources: The elevations of the two models (a) and (b) are used to get the vertical dimension limits of the buildings. The layouts are taken from the OpenStreetMap road map (c). The final results are three dimensional representations of the buildings (d).

In Fig. 3 the generation of the 3D models from the different digital map sources is shown.

As mentioned above, the spatial database extension implements fast and efficient geo-referenced queries which allow real-time processing.

B. Multipath Prediction and Detection

In this section the proposed multipath detection algorithm is described. Furthermore, it is discussed, how the result of the multipath detection can be integrated into standard positioning algorithms.

1) Influence to Localization Algorithm: The standard algorithm for GNSS-positioning uses a weighted least-squares method to estimate a 3D position in ECEF coordinates from a time-synchronized set of pseudoranges [7] . To take the time offset between the local receiver and the satellite system time into account, a fourth unknown— the receiver time offset—needs to be calculated as well. The weights are normally chosen in respect of the signal-to-noise ratio of the measurements or the elevation angle to the satellites. To incorporate the results of the multipath detection, there are two possible solutions:

- Completely exclude suspicious pseudoranges from the observation set. This aggressive approach may lead to less than four pseudorange measurements, which makes a least-squares solution impossible.
- Modify the weights of the suspicious pseudoranges, so that the least-squares method pays less attention to this observations.

Within this paper, the first method—the exclusion of suspicious observations—will be investigated. It should be noted that for a single-GNSS localization algorithm, this approach would be rather radical, as it might result in too less satellites for least-squares solving. The rationale behind this choice is the assumption that for a multi-constellation GNSS algorithm a larger number of satellites is available. Therefore, this strict exclusion is acceptable.

2) Raytracing Model: The simple raytracing model is limited to examine whether a direct line-of-sight between the assumed GNSS antenna position and the GNSS satellites is present. In order to perform this test, the theoretical signal path is tested to intersect with the 3D environmental model from section IV-A. If an intersection of a modeled pseudorange with a building surface is detected, the pseudorange observation is completely excluded from the positioning algorithm as described in section IV-B.1.

3) Probabilistic Distance Model: One major drawback of the simple raytracing model is that it completely ignores uncertainties in the digital maps and the 3D environmental model as well. That is, the building models and the antenna position are assumed to be exactly known, which is not true. One objective of this work was to introduce a lightweight and fault-tolerant multipath detection algorithm, which can explicitly cope with uncertain map information.

In order to perform a probabilistic multipath detection, the raytracing model is extended: Instead of testing only for direct intersections of the theoretical signal path with building surfaces, for each pseudorange the minimum distance x_{min} to all surrounding buildings is determined. In Fig. 4 such a situation is shown. Now the probability $P_{\text{multipath}}$, that a pseudorange has multipath, can be formulated depending on the minimum distance x_{min} present:

$$P_{\text{multipath}} = P(\exists M = \text{true} | x_{\text{min}}) \quad (6)$$

$$P(\exists M = \text{true} | x_{\text{min}}) = 2 \int_{x_{\text{min}}}^{\infty} \mathcal{N}(x,\, 0,\, \sigma^2_{\text{map}})\, \mathrm{d}x. \quad (7)$$

Here, M denotes the binary stochastic variable of multipath which can be *true* or *false*. The probability density function of the event that multipath is present even if a pseudorange not directly intersects a building is modeled as a normal distribution. The free parameter σ_{map} can be used to adapt the multipath detection to different levels of uncertain maps. As indicated above, if the signal path directly intersects the building, it is still more likely that a pseudorange will be subject to multipath. Hence, when x_{min} increases, the pseudorange is assumed more and more multipath free. Depending on the resulting probability and the a priori chosen parameter σ_{map}, now a threshold for the exclusion can be defined.

Fig. 4. The red building on the left side causes a significant multipath to the red pseudorange. The simple raytracing model would not detect this and declare the pseudorange as multipath free. Nevertheless the GNSS observation was subject to multipath which is indicated by the wrong magenta position trajectory (ground truth is shown in green). In contrast, the probabilistic distance model would properly detect this situation and yield the blue trajectory.

V. Evaluation Methodology

A. Simulation and Experimental Setup

The 3D multipath detection algorithm is embedded in the system architecture shown in Fig. 5. A combined GPS and GLONASS receiver constantly measures pseudoranges on the L1 frequency. To validate the multipath detection, two different modes are implemented:

1) Experimental Run: In this mode, the pseudoranges are simply passed from the GNSS receiver to the 3D multipath detection algorithm without any modifications. As no dedicated multipath reference sensor is available, the accuracy of the multipath detection is only assessed indirectly through the positioning error and the integrity.

2) Multipath Simulation: In this mode, the *Multipath Simulator* is actively introducing multipath effects to certain pseudoranges. Therefore, it is exactly known when and for which satellite multipath was present.

B. Evaluation Criteria

The proposed multipath detection algorithm is evaluated with two different methods.

In the simulation mode, the potential multipath detections are compared to the multipath introduced by the simulation at each time step. Afterwards, the total number of correct, missing, and false detections for the complete sequence is known. This procedure is repeated for different uncertainty values of the digital map database.

In the experimental mode, the time when multipath was present depends on the real urban environment during the test drive and is therefore not exactly known. Hence, the multipath detection performance is only indirectly measurable through the decreased positioning error and its higher confidence. The horizontal positioning error is calculated by comparing the Bayes filter results to a ground truth reference trajectory.

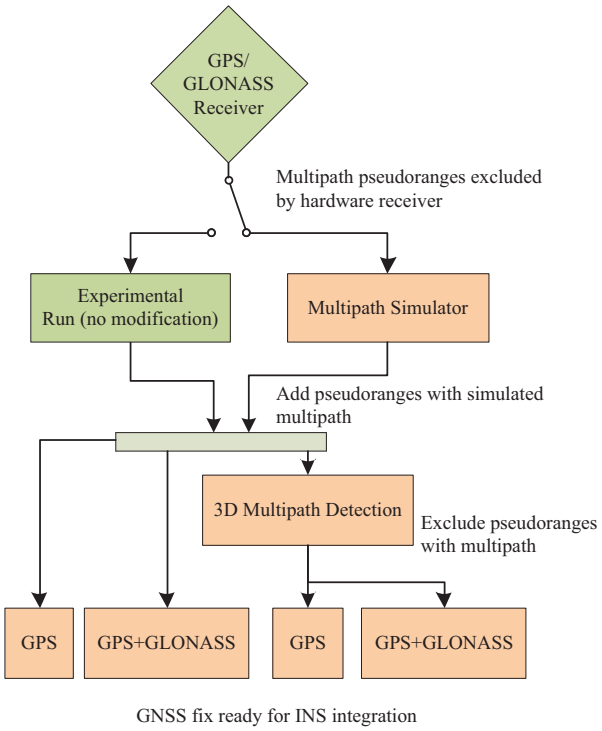

Fig. 5. System setup used for simulation and real data evaluation. The 3D multipath detection algorithm is validated with real data from an urban measurement test drive and simulated multipath.

The positioning performance is evaluated for four different algorithmic combinations:

1) *GPS:* The raw GPS pseudoranges from the GNSS receiver are used to generate a position fix and fused within the loosely-coupled Bayes filter.
2) *GPS+GLONASS:* The pseudoranges from both GNSSs are used to generate a combined position fix and fused with the loosely-coupled Bayes filter.
3) *GPS+3D-MPD:* The raw GPS pseudoranges are filtered by the 3D multipath detection algorithm. The remaining pseudoranges—considered multipath free—are used to generate a position fix. If the number of pseudoranges is smaller than four, no fix calculation is possible and the Bayes filter skips the GNSS measurement update.
4) *GPS+GLONASS+3D-MPD*: All pseudoranges from both GNSSs are passed to the 3D multipath detection. From the remaining pseudorange measurements, a combined GNSS fix is calculated and feed to the Bayes filter.

For each of the above combinations, the true horizontal positioning error is computed and compared to the estimated covariance of the integrated Bayes filter. To account for the positioning needs of different ADAS applications, the percentage of position fixes within the $\sigma, 2\sigma$ and 3σ confidence interval is determined.

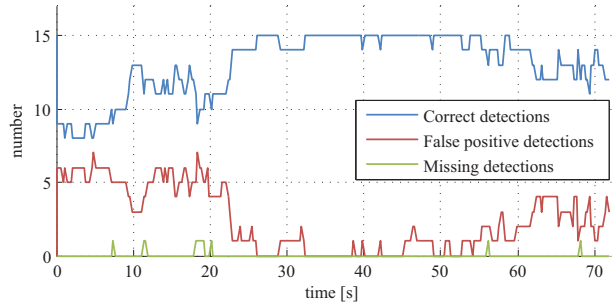

Fig. 6. Result of multipath detection algorithm for the whole test drive sequence compared to known simulation parameters. In this run, a probabilistic range distance σ_{map} of 5 m was configured.

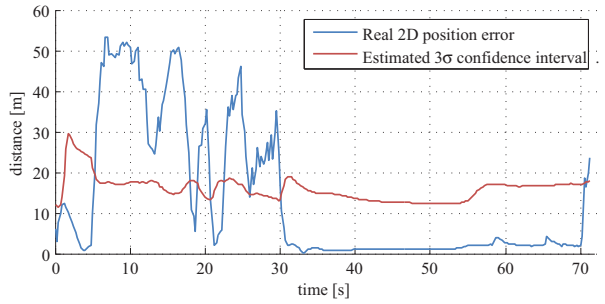

Fig. 7. Positioning error (blue) and estimated σ confidence interval (red) for GPS-only algorithm under multipath conditions. Especially in the first half of the measurement sequence, the position error is underestimated.

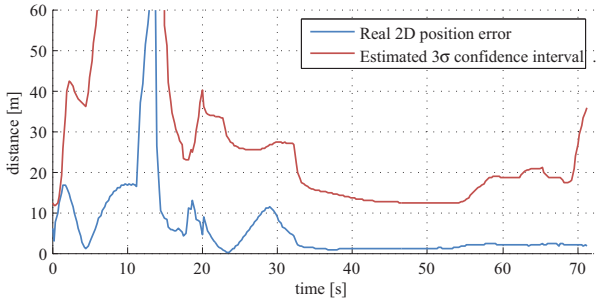

Fig. 8. GPS-only localization with proposed multipath detection algorithm enabled. Multipath affected measurements are identified and the confidence interval is raised appropriately.

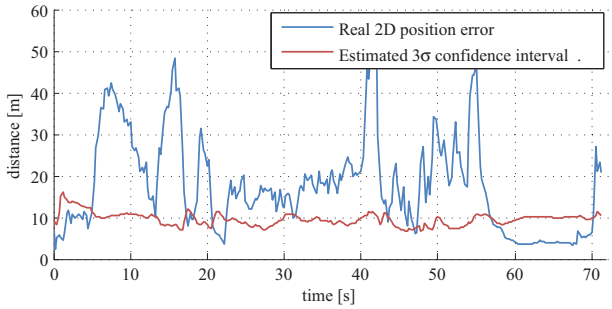

Fig. 9. Result of multi-constellation GNSS algorithm without activated multipath detection. Almost all fixes are outside of the estimated confidence interval.

C. Sensor Configuration

In order to perform the multipath detection algorithm, real experimental data was recorded during a urban test drive using the rapid-prototyping test vehicle *Carai* [13]. The test vehicle was equipped with a NovAtel OEMV GNSS receiver which supports GPS and GLONASS raw observation data. The pseudoranges of both systems were recorded with 10 Hz.

Furthermore the odometry/INS measurements (velocity and yaw rate) of the in-vehicle CAN-bus were recorded with 50 Hz.

Due to the final evaluation of the positioning error, a highly reliable ground truth reference is needed. Therefore, an additional NovAtel SPAN system which integrates GNSS positioning and inertial navigation has been used. It consists of a dual-frequency GPS receiver with Real Time Kinematic (RTK) support. Together with the Honeywell HG1700 inertial measurement unit (IMU), a reliable reference trajectory with sub-decimeter accuracy is achievable.

VI. Quantitative Results

A. Multipath Detections

In order to validate the multipath detection algorithm, it was run in a simulated environment. The simulation used real data to introduce multipath delays at appropriate situations. Table I shows a summary of correct, missing and false detections for different values of the probabilistic range detection parameter σ_{map}. For a range distance of 0.0 m this model is similar to the simple raytracing method described in section IV-B.2. Even if there are about 93 % of successful detections, app. 7 % are completely missed. If the probabilistic range distance parameter is increased—which means the digital map data is assumed more uncertain—the missing detections get lower at the expense of more false positives. Fig. 6 shows the distribution of the performed detections for the whole test drive sequence. Within the interval of the first 25 seconds it can be seen that the multipath detection produced a number of false positive detections, which is caused by wrong map data.

B. Single-constellation Position Error

In Fig. 7 the positioning error and the estimated 3σ confidence interval for a GPS-only localization algorithm

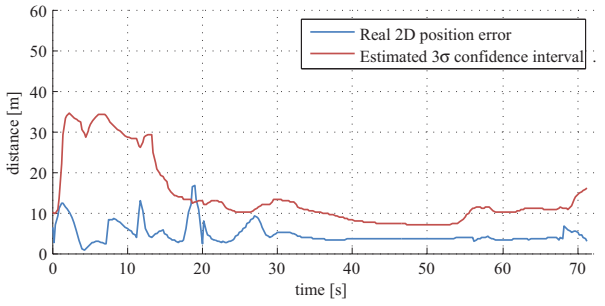

Fig. 10. Multi-constellation GNSS algorithm with multipath detection. The absolute positioning error as well as the confidence is improved significantly.

TABLE I

PERCENTAGE OF CORRECT, MISSING AND FALSE POSITIVE DETECTIONS

Range Distance σ_{map}	Correct	Missing	False
0.0 m	93.3 %	6.7 %	0.0 %
1.0 m	88.8 %	0.3 %	10.9 %
5.0 m	84.0 %	0.2 %	15.8 %

TABLE II

PERCENTAGE OF FIXES WITHIN THE ESTIMATED CONFIDENCE INTERVAL

Algorithm	σ	2σ	3σ	RMSE
GPS	62 %	65 %	68 %	21.4 m
GPS + 3D-MPD	88 %	98 %	99 %	12.2 m
GPS + GLONASS	1 %	20 %	31 %	21.2 m
GPS + GLONASS + 3D-MPD	37 %	94 %	98 %	5.2 m

under multipath is shown. Figure 8 illustrates the same results for a GPS-only algorithm with integrated 3D multipath detection. It can be seen that with the multipath detection algorithm, the confidence interval is more dynamically, i.e. it adapts to local conditions. If the horizontal position raise, the positioning algorithm detects this and automatically increases the estimated covariance as well. As a result, the estimated confidence of the Bayes filter is more appropriate than in the GPS-only case.

C. Multi-constellation Position Error

For the multi-constellation GNSS localization the situation is quite similar. Here, the multipath detection dynamically changes the covariance of the position estimation as well, see Fig. 10. If no multipath detection is used as shown in Fig. 9, the localization algorithm underestimates the positioning error dramatically. Quite all position fixes are now outside the σ confidence interval.

Tabel II contains a summary of all evaluatated positioning algorithms. In all cases, the multipath detection algorithm increases the percentage of fixes within the estimated confidence intervall, while lowering the root mean squared error (RMSE) at the same time.

VII. CONCLUSIONS

This paper attempted to demonstrate a generic and lightweight multipath detection algorithm for multi-constellation GNSS positioning in urban areas. It was shown that a 3D environmental map can be built dynamically in real-time with low computational demands from different digital map data sources. Within this map, potential multipath situations can be predicted and identified through a probabilistic raytracing model. Furthermore, the model proved to be able to cope with uncertain map information through an adjustable parameter. Especially for the simultaneous use of GPS and GLONASS the positioning error and the estimated confidence were optimized. Moreover, the proposed model was successfully integrated into a loosely coupled GNSS/INS positioning algorithm which is heavily used in vehicle localization.

Future work will investigate a benefit analysis of tightly and loosely coupled GNSS/INS approaches when used with the introduced multipath detection model. Additionally, the authors are working on an adaption to other available GNSSs like the European Galileo or Chinese Compass system. Moreover, the replacement of the raytracing step with a multipath shadow map will be investigated.

ACKNOWLEDGMENT

This work was done within the GAIN project. GAIN is a research project co-funded by the European GNSS Supervisory Authority (GSA) in the 7th Framework Programme of the European Commission and is coordinated by Centro Ricerche FIAT. The authors would like to thank GSA for supporting this work. Furthermore, the commitment of the GAIN partners Centro Ricerche FIAT, Magneti Marelli, Chemnitz University of Technology, NAVTEQ Europe, Facit Research GmbH & Co. KG and Instituto Superiore Mario Boella is gratefully acknowledged.

Furthermore, for this evaluation and generation of ground truth data, precise real-time corrections provided by the ascos service (http://www.ascos.de) were used.

REFERENCES

[1] J. Ray, M. Cannon, and P. Fenton, "GPS code and carrier multipath mitigation using a multiantenna system," *IEEE Transactions on Aerospace and Electronic Systems*, vol. 37, no. 1, pp. 183–195, 2001.

[2] Z. Qiang, Z. Xiaolin, and C. Xiaoming, "Research on RAIM Algorithm under the Assumption of Simultaneous Multiple Satellites Failure," *Eighth ACIS International Conference on Software Engineering, Artificial Intelligence, Networking, and Parallel/Distributed Computing (SNPD 2007)*, pp. 719–724, July 2007.

[3] J.-i. Meguro, T. Murata, J.-i. Takiguchi, Y. Amano, and T. Hashizume, "GPS Multipath Mitigation for Urban Area Using Omnidirectional Infrared Camera," *IEEE Transactions on Intelligent Transportation Systems*, vol. 10, no. 1, pp. 22–30, Mar. 2009.

[4] E. Costa, "Simulation of the Effects of Different Urban Environments on GPS Performance Using Digital Elevation Models and Building Databases," *IEEE Transactions on Intelligent Transportation Systems*, pp. 1–11, 2011.

[5] H. Pesonen, "A Framework for Bayesian Receiver Autonomous Integrity Monitoring in Urban Navigation," in *NAVIGATION*, vol. 58, no. 3, 2011, pp. 229–240.

[6] P. G. Mattos, "Accuracy and availability trials of the consumer gps/glonass receiver in highly obstructed environments," in *Proceedings of the 24th International Technical Meeting of The Satellite Division of the Institute of Navigation (ION GNSS 2011)*, Oregon Convention Center, Portland, Oregon, September 2011, pp. 2740–2744.

[7] E. Kaplan and C. Hegarty, *Understanding GPS: principles and applications*. Artech House Publishers, 2006.

[8] L. Xu, X. Li, and Y. Xue, "Two methods of processing system time offset in multi-constellation integrated system," in *Electrical Engineering and Control*, ser. Lecture Notes in Electrical Engineering, M. Zhu, Ed. Springer Berlin Heidelberg, 2011, vol. 98, pp. 359–365.

[9] R. Schubert, C. Adam, M. Obst, N. Mattern, V. Leonhardt, and G. Wanielik, "Empirical evaluation of vehicular models for ego motion estimation," 2011.

[10] S. J. Julier and J. K. Uhlmann, "Unscented filtering and nonlinear estimation," *Proceedings of the IEEE*, vol. 92, no. 3, pp. 401–422, March 2004.

[11] R. Schubert, *Integrated Bayesian Object and Situation Assessment for Lane Change Assistance*. Shaker Verlag, 2011.

[12] OpenStreetMap Wiki, "Shapefiles," last checked: 25.10.2011. [Online]. Available: http://wiki.openstreetmap.org/wiki/Shapefiles

[13] R. Schubert, E. Richter, N. Mattern, P. Lindner, and G. Wanielik, *Advanced Microsystems for Automotive Applications 2010*. Springer, 2010, ch. A Concept Vehicle for Rapid Prototyping of Advanced Driver Assistance Systems, pp. 211–219.